Metamodel-based adaptive use of a coherent polarimetric backscattering simulator for the characterization of forested areas at low frequencies

Andras Vasko, Laetitia Thirion-Lefèvre, Sandór Bilicz, Isabelle Champion, Marc Lambert, Szabolcs Gyimothy

Metamodel-based Adaptive Use of a Coherent Polarimetric Backscattering Simulator for the Characterization of Forested Areas at Low Ffrequencies

A. Vasko[1,4], L. Thirion-Lefevre[2], S. Bilicz[1,4], I. Champion[3], M. Lambert[1], and S. Gyimóthy[4]

[1]L2S, UMR 8506, CNRS-SUPELEC, University Paris-Sud, France
[2]SONDRA/SUPELEC, France
[3]EPHYSE/INRA, France
[4]Budapest University of Technology and Economics, Hungary

Abstract— We present a new method for forest characteristics inversion, based on a surrogate model derived from a full wave electromagnetic simulator using kriging techniques. To illustrate the feasibility of this method, we consider a simple configuration for the forest and we use the polarimetric backscattering coefficients to retrieve both the age of the trunks and the ground moisture with different frequency bands. The benefit of polarimetry in this retrieval process is then studied.

1. INTRODUCTION

In the frame of forest observation, e.g., in the purpose of biomass retrieval, simple scattering models are used to perform inversion. For instance, the Random Volume over Ground (RVoG) model [1] derived from the work of Treuhaft et al. [2] is widely used to retrieve the mean height of the forest (see [3, 4]). However, the use of more complex scattering models (such as COSMO in [5]) for inversion appears to be difficult due to several bottlenecks, such as the high number of descriptive parameters and the computational cost of the simulation.

In this paper, we propose the combined use of a coherent polarimetric backscattering simulator and some adaptive metamodeling tools, which have already been used in electromagnetic nondestrucive evaluation (e.g., [6]). We present the metamodeling tools and the surrogate model derived from the coherent polarimetric backscattering simulator (COSMO). Considering a set of polarimetric backscattering coefficients obtained for a given radar configuration and derived from the backscattered fields, we address the inverse problem of determining the forest age and the ground moisture by using the surrogate model. The impact of the radar parameters (frequency, incidence angle and also with special attention to the number of polarimetric channels) is investigated, namely to evaluate the accuracy we can expect on the retrieved quantities.

In the numerical study, we consider the case of a French temperate managed forest whose structure and radar response have already been widely studied in [5] and [7], respectively. For the illustration of the ability of the metamodeling tools to perform inversion, we propose herein to focus on a simple description of the forest: only the dielectric trunks standing on a rough and dielectric surface are considered. This can be seen as a rough, but acceptable approximation at the frequencies considered.

2. METAMODELING BY KRIGING

The main objective of metamodeling (or surrogate modeling) is to make a cheap-to-evaluate approximation for the response of a given, usually complex numerical simulator. For a formal description, let us denote the numerical simulation by the so-called forward operator $\mathcal{F}$:

$$\mathcal{F}\{\mathbf{x}\} = y_{\mathbf{x}}(\mathbf{t}) \qquad \mathbf{x} \in \mathbb{X}, \mathbf{t} \in \mathbb{T}, \tag{1}$$

where $\mathbf{x}$ is the vector of input variables and the output (response) of the forward operator is a function of the $\mathbf{t}$ parameter. In our case, $\mathbf{x} = [a, m_v]^\mathsf{T}$ is the forest age a and ground moisture m_v, whereas $\mathbf{t} = [f, \theta]^\mathsf{T}$ is the applied frequency and incidence angle in the measurement setup. The domain $\mathbb{X}$ is called the input space, whereas $\mathbb{T}$ is the set of all feasible measurement parameters.

A common way of metamodeling is to evaluate the forward operator at certain values of the input parameters and to use interpolation to approximate the response at any unobserved values. Obviously, both the interpolator and the choice of the points where the forward operator is evaluated, highly influence the performance of the metamodel. In our study, we use the kriging technique [8] for interpolation, and the evaluation points are adaptively chosen.

2.1. Kriging Interpolation

Traditionally, kriging has been used to interpolate scalar functions, however, our forward operator yields functional data, thus a recent extension —called functional kriging, [9] — is used for this purpose. Functional kriging models the output data $y_{\mathbf{x}}(\mathbf{t})$ by a functional Gaussian random process $Y_{\mathbf{x}}(\mathbf{t})$, and the observations are treated as its samples. Kriging then computes a linear prediction of the random process based on the set of samples $Y_1(\mathbf{t}), Y_2(\mathbf{t}), \ldots, Y_n(\mathbf{t})$ at the points $\mathbf{x}_1, \mathbf{x}_2, \ldots, \mathbf{x}_n$ as $\hat{Y}_{\mathbf{x}}(\mathbf{t}) = \sum_{i=1}^{n} \lambda_i(\mathbf{x}) Y_i(\mathbf{t})$, where the coefficients $\lambda_i(\mathbf{x})$ are computed in a closed form based on the covariance of the modeling process, satisfying the criterion

$$s^2(\mathbf{x}) = \int_{\mathbb{T}} \mathbb{E}\left[\left(\hat{Y}_{\mathbf{x}}(\mathbf{t}) - Y_{\mathbf{x}}(\mathbf{t})\right)^2\right] \mathrm{d}\mathbf{t} \rightarrow \text{the smallest, s.t. } \mathbb{E}\left[\hat{Y}_{\mathbf{x}}(\mathbf{t}) - Y_{\mathbf{x}}(\mathbf{t})\right] = 0, \quad \forall \mathbf{x} \in \mathbb{X}, \qquad (2)$$

where $s^2(\mathbf{x})$ is the so-called trace variance and $\mathbb{E}$ stands for the expected value operator.

2.2. Adaptive Sampling

The performance of the kriging prediction obviously depends on the choice of the samples. The sample set should thus be an ideal discrete representation of the forward operator. Since we do not have any prior information on the behaviour of the latter, an adaptive sampling algorithm is needed. Our method is based on the step-by-step reduction of the uncertainty of the kriging prediction. The algorithm — presented in detail in [6] — consists in the following steps:

1. Choose n initial sample points in $\mathbb{X}$ and evaluate $\mathcal{F}$ there. These points are selected with the classical sampling method called the full-factorial sampling (i.e., in the nodes of regular grid);
2. Compute the kriging prediction over the input space based on the $y_1(\mathbf{t}), y_2(\mathbf{t}), \ldots, y_n(\mathbf{t})$ samples by computing the optimal coefficients $\lambda_i(\mathbf{x})$ and substituting the observations of the modeling process $Y_i(\mathbf{t})$ by the corresponding sample $y_i(\mathbf{t})$;
3. Find the next sample point as $\mathbf{x}_{n+1} = \arg\max_{\mathbf{x}\in\mathbb{X}} (\hat{s}^2(\mathbf{x}) \min_{i=1,\ldots,n} \|\mathbf{x} - \mathbf{x_i}\|)$. The first factor $\hat{s}^2(\mathbf{x})$ is the variance from (2) predicted with the jackknife variance estimation, referring to the uncertainty of the prediction. The second factor is the Euclidean distance to the nearest sample in $\mathbb{X}$, introduced to enforce the balanced filling of $\mathbb{X}$ by samples;
4. Add $y_{n+1}(\mathbf{t}) = \mathcal{F}\{\mathbf{x}_{n+1}\}$ to the sample set, and increase n to $n+1$;
5. Go to step 2 until n reaches a given value.

2.3. Validation of the Model

In the frame of our studies, the forward operator yields the polarimetric backscattering coefficient, i.e., $\mathcal{F}\{\mathbf{x}\} = \sigma_p^{\mathbf{x}}(f,\theta)$ where p is the polarization channel (either VV, VH or HH). The goal of the metamodel generation is to find a good approximation of $\mathcal{F}$ based on the $\sigma_p^{\mathbf{x}}(f,\theta)$ functional observations. In our numerical studies, the $\sigma_p^{\mathbf{x}}(f,\theta)$ functions are represented by a finite number of samples obtained at certain (f,θ) values. For a proper representation, these scalar samples of each $\sigma_p^{\mathbf{x}}(f,\theta)$ function are also adaptively chosen, i.e., a two-level adaptive sampling strategy is used. The *upper* level is the sampling of $\mathcal{F}$, where the observations are the $\sigma_p^{\mathbf{x}}(f,\theta)$ *functions*, i.e., the sampling aims at choosing the best $\mathbf{x}$ samples. The *lower* level is responsible for the representation of a *particular* $\sigma_p^{\mathbf{x}}(f,\theta)$ function by the optimal choice of the (f,θ) values. Both levels use the same adaptive sampling algorithm introduced in Section 2.2 but with different objective functions.

To illustrate the efficiency of the two-level adaptive sampling method, we compare the result of this method with a metamodel that was generated with a regular sampling. The mean interpolation error is calculated as $\varepsilon_p(\mathbf{x}) = \sqrt{\frac{1}{\Delta f \Delta\theta} \int_{f_0}^{f_1} \int_{\theta_0}^{\theta_1} [\hat{\sigma}_p^{\mathbf{x}}(f,\theta) - \sigma_p^{\mathbf{x}}(f,\theta)]^2 \mathrm{d}\theta \mathrm{d}f}$. The results are presented in Fig. 1: the adaptive metamodel seems to outperform the regular one.

3. APPLICATION TO THE RETRIEVAL OF AGE AND GROUND MOISTURE

In this paper, we study the radar backscattering response of the Nezer forest, a pine trees forest, that has been widely described [7]. Its allometric equations have been derived [10], implying that we can describe it with a few parameters. Thus, it is now possible to retrieve some descriptive quantities of the forest using some radar observables. In a previous study [11], we have worked

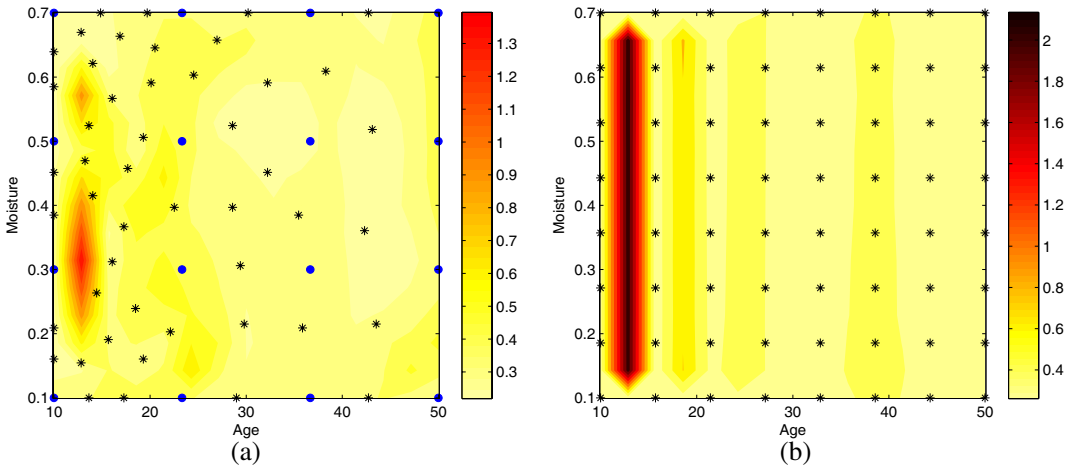

Figure 1: Interpolation error $\varepsilon(\mathbf{x})$ of the adaptive and the regular metamodel. Both consist in 64 samples in the input space, and each sample is represented by 64 pairs of (f, θ). The regular model uses 8×8 grids in both levels. The true values are computed on fine grids (involving totally 45200 simulations). (a) Adaptive metamodel (dots: initial samples, stars: sequentially added samples). (b) Regular metamodel.

with the polarimetric backscattering coefficients, the polarimetric interferometric heights, and the attenuation for the co-polarizations. In addition, we have simulated a whole forest (ground, trunks and branches), but for a given age of the forest and a constant gravimetric ground moisture m_v only. In order to illustrate the feasibility of our method, we consider here a simple forest configuration and we only use the polarimetric backscattering coefficients.

For simplicity, the forest under study is described only by its trunks. These trunks are modeled as almost vertical dielectric cylinders standing on a dielectric and rough ground. The age (a) of the trunks varies between 10 and 50 years: each age corresponds to a height h and a diameter d (in meters). These quantities are derived using the allometric equations presented in [10]: $h = 56.618 \times d + 0.646$ with $d = 0.169 \times \log(a) - 0.257$. The moisture of the trunks and the branches is assumed to be constant and around 0.54, the trees density is assumed also to be constant and regularly spaced (5 m distance, see [5] for details). As a consequence, two data are required to describe our scene: the age of the trees and the ground moisture m_v, which is assumed to vary between 0.1 and 0.7. The reference values of the polarimetric backscattering coefficients (σ) are calculated with COSMO. The inversion is performed with our metamodel (Section 2.2). This example is simple as we actually need only two parameters to represent our simple forest. However, it is not expected to be the best case for the illustration of the benefit of polarimetry. Indeed, as the scatterers types are reduced, the polarimetric variety is weak.

To analyse the performance of inversion, we have selected four representative examples: the age is either 20 or 40 years and the ground moisture is equal either to 0.25 or 0.55. We present first error maps and then we comment some of our results.

3.1. Introduction to Error Maps

In Fig. 2, we have plotted four error maps, that represent the errors we obtained both on the retrieved m_v and a using σ. In this example, $a = 40$ years and $m_v = 0.25$. Radar measurements between 1 GHz and 2 GHz and incidence angles between 59° and 61° are assumed. The white stars indicate for each polarization, the location of the true point $(a = 40, m_v = 0.25)$, σ being given for information. We observe in Fig. 2, that the best polarimetric channel (BPC) is VH (Fig. 2(b)), but we need the additional information brought both by VV and HH to obtain a better result (called CPC, for Combined Polarimetric Channels) (Fig. 2(d)). The drawn boxes represents the boundaries considered for inversion assuming an error of 1 dB. In this example, VH channel allows to estimate a such as $a \in [37, 41]$. There is an ambiguity on m_v and we can only estimate that $m_v \in \{[0.14, 0.41] \cup [0.48, 0.7]\}$, that is clearly not satisfying. When combining the full polarimetric information, the estimation of m_v is improved ($m_v \in [0.17, 0.39]$).

3.2. A Focus on the Impact of Polarimetry on the Retrieval of a and m_v

In this section, we investigate the role of polarimetry in the inversion of the trunks age and the ground moisture. It is obvious that the scattering mechanisms evolve with the frequency and so do the polarimetric mechanisms. As a consequence, we do not expect the same benefit of polarimetric

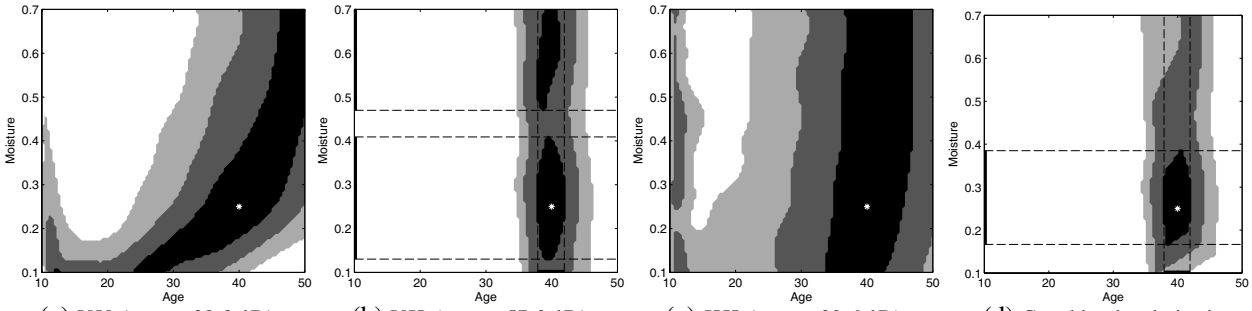

Figure 2: Illustration of error maps for $(a = 40, m_v = 0.25)$, frequency bandwidth=$[1000, 2000]$ MHz and incidence angle range = $[59, 61]°$. Black area refers to an error less than 1 dB, dark grey one to an error between 1 dB and 2 dB, and the light grey one between 2 dB and 3 dB. Boxes represent the boundaries we consider for inversion: VH is classified in this example as the best polarimetric channel.

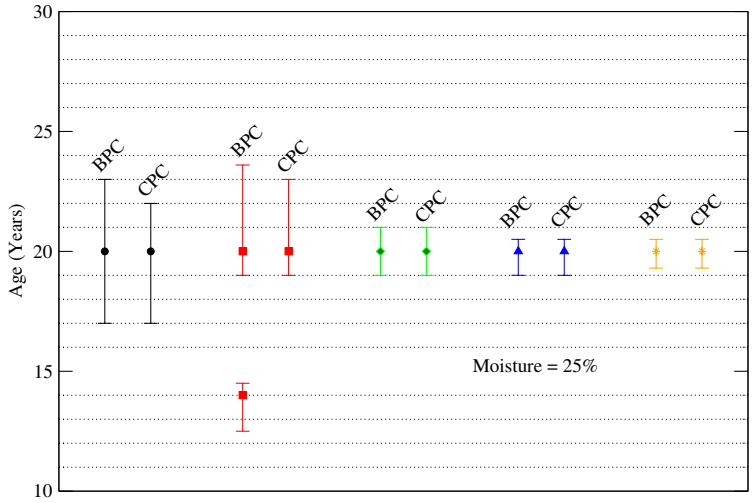

Figure 3: Age retrieval for different frequency bands and different polarimetric arrangements. The case to retrieve is $(a = 20, m_v = 0.25)$. For each frequency range, there are two cases: the best polarimetric channel results (BPC) either VV, HH or HV polarization; the combined polarimetric channels results (CPC) considering the three polarimetric channels. The bars represent the interval error.

information depending on the frequency range we consider. Therefore, we have defined five cases arranged in three groups: (1) some usual radar configurations $[400, 470]$ MHz (•) and $[1230, 1350]$ MHz (□); (2) enlarged low and hight frequency bands $[350, 1000]$ MHz) (◊) and $[1000, 2000]$ MHz (△) respectively; and finally (3) the whole frequency range, $[350, 2000]$ MHz (*).

3.2.1. Age Retrieval

In Fig. 3, we observe that polarimetric information does not contribute significantly to the inversion of the age. Error bars are about the same, either when considering the BPC or the CPC. On the contrary, the frequency range seems crucial: the larger it is, the more accurate is the retrieval of a. This trend is confirmed by additional results for other a and m_v, except that considering the whole frequency range does not always lead to the best case. However, as illustrated with the frequency range $[1230, 1350]$ MHz (□), ambiguities may appear: is $a \in [13, 15]$ or $a \in [19, 24]$? Using CPC allows to suppress this uncertainty and even gives a little more accuracy with $a \in [19, 23]$.

3.2.2. Moisture Retrieval

For m_v retrieval (Fig. 4(a)), the roles of the frequency ranges and the polarimetry are not the same, a clear benefit of polarimetry enabling to suppress ambiguities and reducing significantly the error interval is shown. However, the quality of the inversion is not comparable: in the cases we have considered it is obviously more difficult to retrieve the ground moisture than the dimensions of the trunks. The additional results we obtained (see, e.g., Fig. 4(b)) lead us to think that polarimetry is mandatory when we do not obtain more accurate results with larger frequency range.

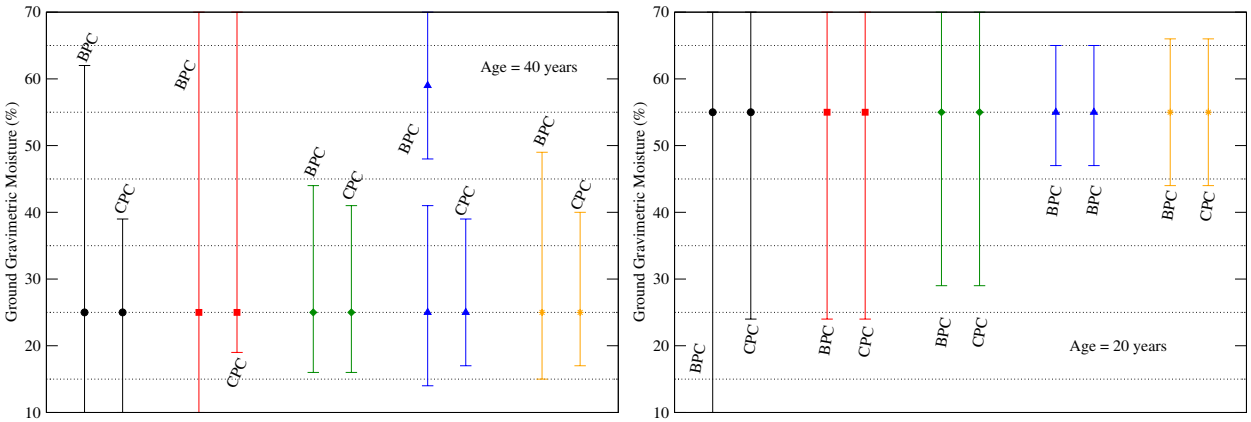

(a) $a = 40, m_v = 0.25$ (b) $a = 20, m_v = 0.55$

Figure 4: Ground moisture retrieval for different frequency bands and different polarimetric arrangements.

4. CONCLUSION

We have presented in this paper a new method for forest characteristics inversion. We have considered a simple configuration for the forest, that is not considered as the best one to illustrate the benefit of polarimetry. We have used the polarimetric backscattering coefficients to retrieve both the age of the trunks and the ground moisture with different frequency bands. We have produced error maps, that illustrate the uncertainty we obtain and we have studied some examples. The very first results we have obtained lead us to conclude that we cannot state that only one polarimetric channel is sufficient to retrieve correctly our parameters. Actually, it dramatically depends on the variety of the measured scattering mechanisms. This variety is brought for instance by polarimetry or by frequency. But even in the case where the frequency range is large enough to provide this diversity, ambiguities may still remain, that require polarimetry in order to be suppressed.

REFERENCES

1. Cloude, S. R. and K. P. Papathanassiou, "Three-stage inversion process for polarimetric SAR interferometry," *Proc. Inst. Elect. Eng. Radar, Sonar Navig.*, Vol. 150, 125–134, 2003.
2. Treuhaft, R. N., S. Madsen, M. Moghaddam and J. J. van Zyl, "Vegetation characteristics and underlying topography from interferometric data," *Radio Sci.*, Vol. 31, 1449–1485, 1996.
3. Garestier, F., P. Dubois-Fernandez, and K. P. Papathanassiou, "Pine forest height inversion using single-pass X-band Pol-InSAR data," *IEEE Trans. Geosci. Remote Sens.*, Vol. 46, 59–68, 2008.
4. Garestier, F., P. Dubois-Fernandez, and I. Champion, "Forest height inversion using high-resolution P-band Pol-InSAR data," *IEEE Trans. Geosci. Remote Sens.*, Vol. 46, 3544–3559, 2008.
5. Thirion, L., E. Colin, and C. Dahon, "Capabilities of a forest coherent scattering model applied to radiometry, interferometry and polarimetry at P- and L-bands," *IEEE Trans. Geosci. Remote Sens.*, Vol. 44, 849–862, 2006.
6. Bilicz, S., S. Gyimóthy, M. Lambert, and J. Pávó, "Adaptive kriging metamodels for expensive-to-run electromagnetic simulations," *Proc. 14th International IGTE Symposium on Numerical Field Calculation in Electrical Engineering*, 214–219, IGTE, Graz, Austria, 2010.
7. Sartore, M., et al., "Tree architecture in remote sensing analytical models: The Bray experiment," *Int. J. Remote Sens.*, Vol. 22, 1827–1843, 2001.
8. Chilès, J. and P. Delfiner, *Geostatistics, Modeling Spatial Uncertainty*, Wiley, 1999.
9. Delicado, P., R. Giraldo, C. Comas, and J. Mateu, "Statistics for spatial functional data: some recent contributions," *Environmetrics*, Vol. 21, 224–239, 2009.
10. Saleh, K., et al., "A forest geometric description of a Maritime pine forest suitable for discrete microwave models," *IEEE Trans. Geosci. Remote Sens.*, Vol. 43, 2024–2035, 2005.
11. Thirion-Lefevre, L., S. Bilicz, M. Lambert, and Sz. Gyimóthy, "On the use of an *optimal* database for radar forest observation," *8th European Conference on Synthetic Aperture Radar (EUSAR 2010)*, 873–876, 2010.